Journal of Rock Mechanics and Geotechnical Engineering 10 (2018) 968–976

Contents lists available at ScienceDirect

Journal of Rock Mechanics and Geotechnical Engineering

journal homepage: www.rockgeotech.org

Full Length Article

Pullout behavior of polymeric strip in compacted dry granular soil under cyclic tensile load conditions

Sajad Razzazan [a], Amin Keshavarz [a,*], Mansour Mosallanezhad [b]

[a] School of Engineering, Persian Gulf University, Bushehr, Iran
[b] Department of Civil and Environmental Engineering, Shiraz University, Shiraz, Iran

ARTICLE INFO

Article history:
Received 5 December 2017
Received in revised form
9 March 2018
Accepted 13 April 2018
Available online 28 June 2018

Keywords:
Geosynthetics
Post-cyclic pullout behavior
Interface apparent coefficient of friction
Multistage pullout (MSP) test

ABSTRACT

Assessment of the reinforcement behavior of soil under cyclic and monotonic loads is of great importance in the safe design of mechanically stabilized earth walls. In this article, the method of conducting a multistage pullout (MSP) test on the polymeric strip (PS) is presented. The post-cyclic behavior of the reinforcement can be evaluated using a large-scale pullout apparatus adopting MSP test and one-stage pullout (OSP) test procedures. This research investigates the effects of various factors including load amplitude, load frequency, number of load cycles and vertical effective stress on the peak apparent coefficient of friction mobilized at the soil-PS interface and the pullout resistance of the PS buried in dry sandy soil. The results illustrate that changing the cyclic tensile load frequency from 0.1 Hz to 0.5 Hz does not affect the pullout resistance. Moreover, the influence of increasing the number of load cycles from 30 to 250 on the peak pullout resistance is negligible. Finally, the effect of increasing the cyclic tensile load amplitude from 20% to 40% on the monotonic pullout resistance can be ignored. The peak apparent coefficient of friction mobilized at the soil-PS interface under monotonic and cyclic load conditions decreases with the increase in vertical effective stress.

1. Introduction

Polymeric strip (PS) is a type of geosynthetics which is frequently used in mechanically stabilized earth walls (MSEWs). By considering the failure mechanisms in the MSEWs, direct shear and pullout tests are performed to investigate the soil-reinforcement interaction behavior (Palmeira, 2009). In the pullout conditions, the length of reinforcement which is located behind the rupture surface (anchorage length) is tested because the interaction is mobilized in this area. Several studies have been done on these strips such as Lo (1998, 2003). In these two studies, the behavior of PS was evaluated under monotonic conditions. The behaviors of other types of reinforcements under monotonic conditions have been evaluated by several researchers. Palmeira (2004) used numerical and experimental approaches to evaluate the soil-geogrid interaction. Abdi and Arjomand (2011) performed the pullout tests to study the interaction of clays reinforced with geogrids encapsulated in thin layers of sand. Esfandiari and Selamat (2012) carried out the pullout tests on metal strips with transverse members, in combination with π-Buchingham theorem and statistical analysis. Suksiripattanapong et al. (2013) studied the influences of soil properties, dimension and spacing of the transverse members on the pullout mechanism of the bearing reinforcement which is composed of a longitudinal member and a set of transverse members. Alam et al. (2014) investigated the pullout behavior of a steel grid reinforcement using experimental and numerical approaches. In order to increase the pullout resistance of the steel strip, Mosallanezhad et al. (2015) introduced a novel reinforcing element which is composed of a series of extra elements (anchors) attached to the conventional steel strip. Mosallanezhad et al. (2017) introduced a new and simple reinforcement system including transverse geogrids connected to a base geogrid with a 45° angle. They conducted the large-scale pullout tests to evaluate the performance of this reinforcement for increase in pullout resistance.

Moraci and Cardile (2009) conducted a multistage pullout (MSP) test to study the influence of various factors including cyclic tensile load frequency and amplitude, vertical effective stress and tensile stiffness of the geogrid on the post-cyclic pullout resistance. The

* Corresponding author.
E-mail addresses: keshavarz@pgu.ac.ir, amin_keshavarz@yahoo.com (A. Keshavarz).

Peer review under responsibility of Institute of Rock and Soil Mechanics, Chinese Academy of Sciences.

https://doi.org/10.1016/j.jrmge.2018.04.007

Table 1
Specifications of the polymeric strip provided by the manufacturer.

Ultimate tensile strength (kN)	Strip width (mm)	Strip mass (kg/100 m)	Strip length (mm)
75.4	90 ± 2	25.6	700

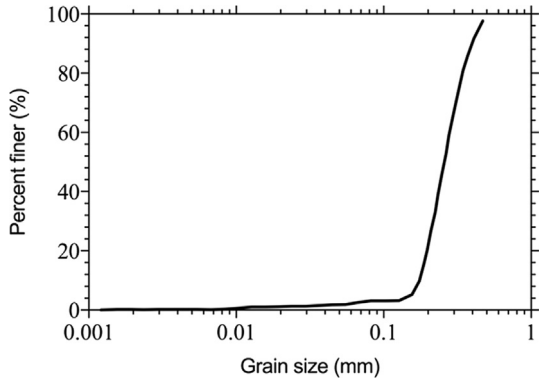

Fig. 1. Particle size distribution curve of the soil.

geogrid was surrounded by granular soils. Their results depicted that the effect of the cyclic tensile load frequency on the test results is negligible. Furthermore, the cyclic tensile load amplitude at the vertical effective stresses greater than 50 kPa affects the pullout resistance, and it can be ignored at the lower vertical effective stresses (e.g. 10 kPa and 25 kPa).

Design methods for the MSEWs subjected to static loading are relatively well studied. But the behavior of embedded geosynthetics subjected to repeated loadings is rarely reported. Such research is required to improve the design of MSEWs under traffic and seismic loading conditions. Moreover, in order to study the internal stability of the MSEWs subjected to cyclic loads, it is essential to estimate the pullout resistance and the interface apparent coefficient of friction mobilized in the anchorage zone. Thus, the behavior of these types of reinforcements under cyclic conditions is important for the safe design. In addition, in many situations, the cause of rupture of MSEWs is the lack of seismic considerations in the design (Ling et al., 2001). Furthermore, these

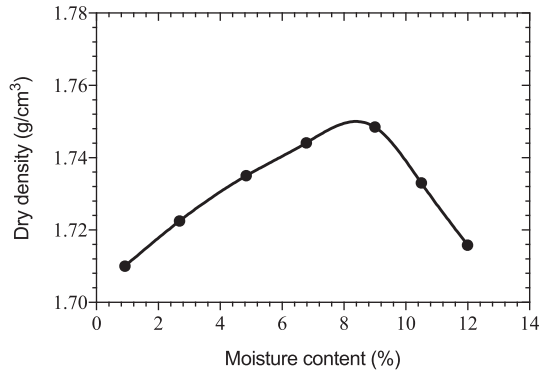

Fig. 2. Compaction curve of the soil.

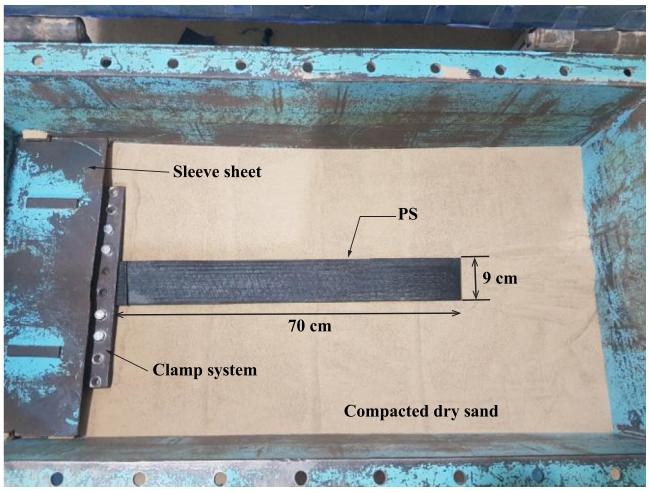

Fig. 3. Placement of strip, clamp system and sleeve sheet in the laboratory.

walls are exposed to different types of loads, such as dead loads, repeated loads caused by vehicle traffic, impact loads caused by compaction of soil layers, and earthquake loads. Therefore, a number of researches have been done on reinforcing systems over the past two decades (Cai and Bathurst, 1995; Ling et al., 1997; Bathurst and Hatami, 1998; Nouri et al., 2006; Nova-Roessig and Sitar, 2006; Latha and Krishna, 2008; Moraci and Cardile, 2012; Tang et al., 2013; Liu et al., 2015; Panah et al., 2015; Cardile et al., 2017).

In general, the pullout resistance at different levels of reinforcement is expressed by the following equation:

$$P_r = F^* \alpha \sigma'_v Lp \tag{1}$$

where P_r is the pullout force, F^* is the coefficient of pullout resistance, α is the scale correction factor, σ'_v is the vertical effective stress in the reinforcement level, p is the section perimeter of the strip, and L is the anchorage length.

The post-cyclic pullout resistance (P_{rc}) and monotonic pullout resistance (P_{rm}) are equal to the shear forces mobilized along the reinforcement:

$$P_{rc} = \tau_{ac} Lp \tag{2}$$

$$P_{rm} = \tau_{am} Lp \tag{3}$$

where τ_{am} and τ_{ac} are the average apparent shear stresses under monotonic and post-cyclic conditions, respectively. Using Eqs. (1)–(3), the relationships between shear stresses and σ'_v are obtained as

$$\tau_{ac} = \mu^c_{s/GSY} \sigma'_v \tag{4}$$

$$\tau_{am} = \mu_{s/GSY} \sigma'_v \tag{5}$$

where $\mu_{s/GSY}$ and $\mu^c_{s/GSY}$ are the monotonic and post-cyclic peak apparent coefficients of friction mobilized at the soil-PS interface, respectively.

Table 2
Soil properties.

D_{10} (mm)	D_{30} (mm)	D_{60} (mm)	c_u	c_c	Composition (%)			Soil classification		G_s	e_{max}	e_{min}
					Fines passing #200 sieve	Sand	Gravel	USCS	AASHTO			
0.15	0.19	0.27	1.8	0.89	4	96	0	SP	A-2-4 (0)	2.65	0.87	0.55

Note: c_u - uniformity coefficient; c_c - coefficient of curvature; G_s - specific gravity; e_{max} - maximum void ratio; e_{min} - minimum void ratio.

Table 3
Summary of pullout test programs.

Test type	Investigated factor	L (cm)	σ'_v (kPa)	f (Hz)	A/P_{rm}	N
MSP	Load frequency (f)	70	20	0.1	0.3	30
		70	20	0.2	0.3	30
		70	20	0.5	0.3	30
		70	30	0.1	0.3	30
		70	30	0.2	0.3	30
		70	30	0.5	0.3	30
	Load amplitude (A)	70	20	0.1	0.2	30
		70	20	0.1	0.4	30
		70	30	0.1	0.2	30
		70	30	0.1	0.4	30
		70	40	0.1	0.2	30
		70	40	0.1	0.3	30
		70	40	0.1	0.4	30
		70	80	0.1	0.2	30
		70	80	0.1	0.3	30
		70	80	0.1	0.4	30
	Number of load cycles (N)	70	20	0.1	0.3	50
		70	20	0.1	0.3	100
		70	20	0.1	0.3	250
		70	30	0.1	0.3	50
		70	30	0.1	0.3	100
		70	30	0.1	0.3	250
OSP	Clamp resistance		20			
			30			
			40			
			80			
	PS resistance	70	20			
		70	30			
		70	40			
		70	80			

As mentioned before, several studies have been carried out on the post-cyclic pullout resistance of reinforcements. However, to the best of the authors' knowledge, few MSP tests have been carried out on the PS. Therefore, the cyclic behavior of this system requires further investigation. In this paper, large-scale pullout tests were used to investigate the factors affecting the post-cyclic behavior of the PS in the compacted dry granular soil. The effects of different factors such as load frequency (f), load amplitude (A), number of load cycles (N), and vertical effective stress on the pullout resistance and the value of $\mu_{s/GSY}$ have been investigated.

2. Experimental studies

2.1. Apparatus and instrumentation

The pullout test device was developed in accordance with ASTM D6706-03 (2003) with a length of 1200 mm, a width of

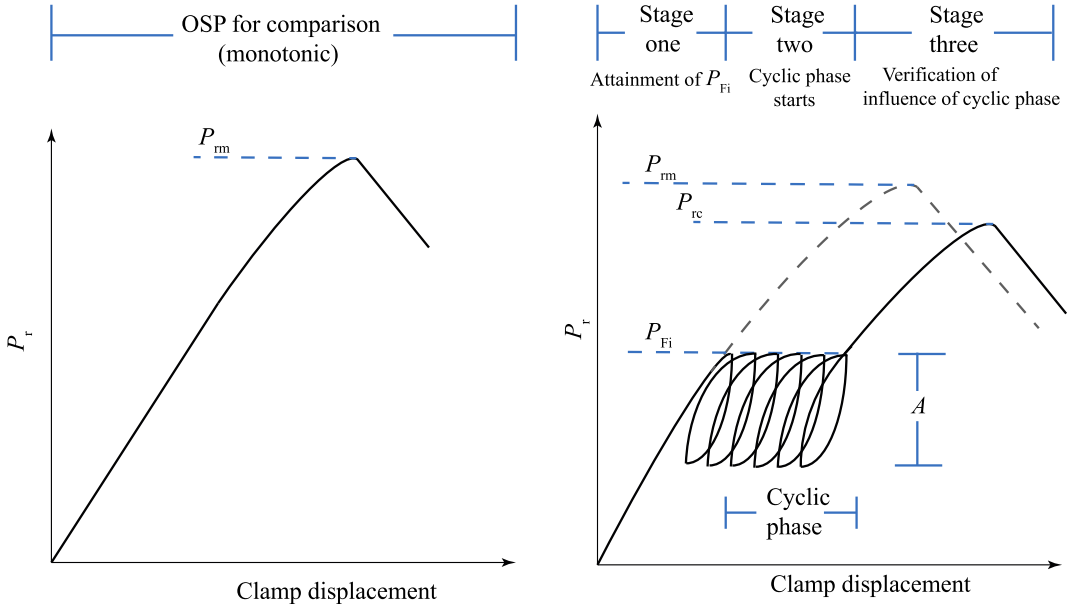

Fig. 4. Schematic representation of one-stage and multistage pullout tests.

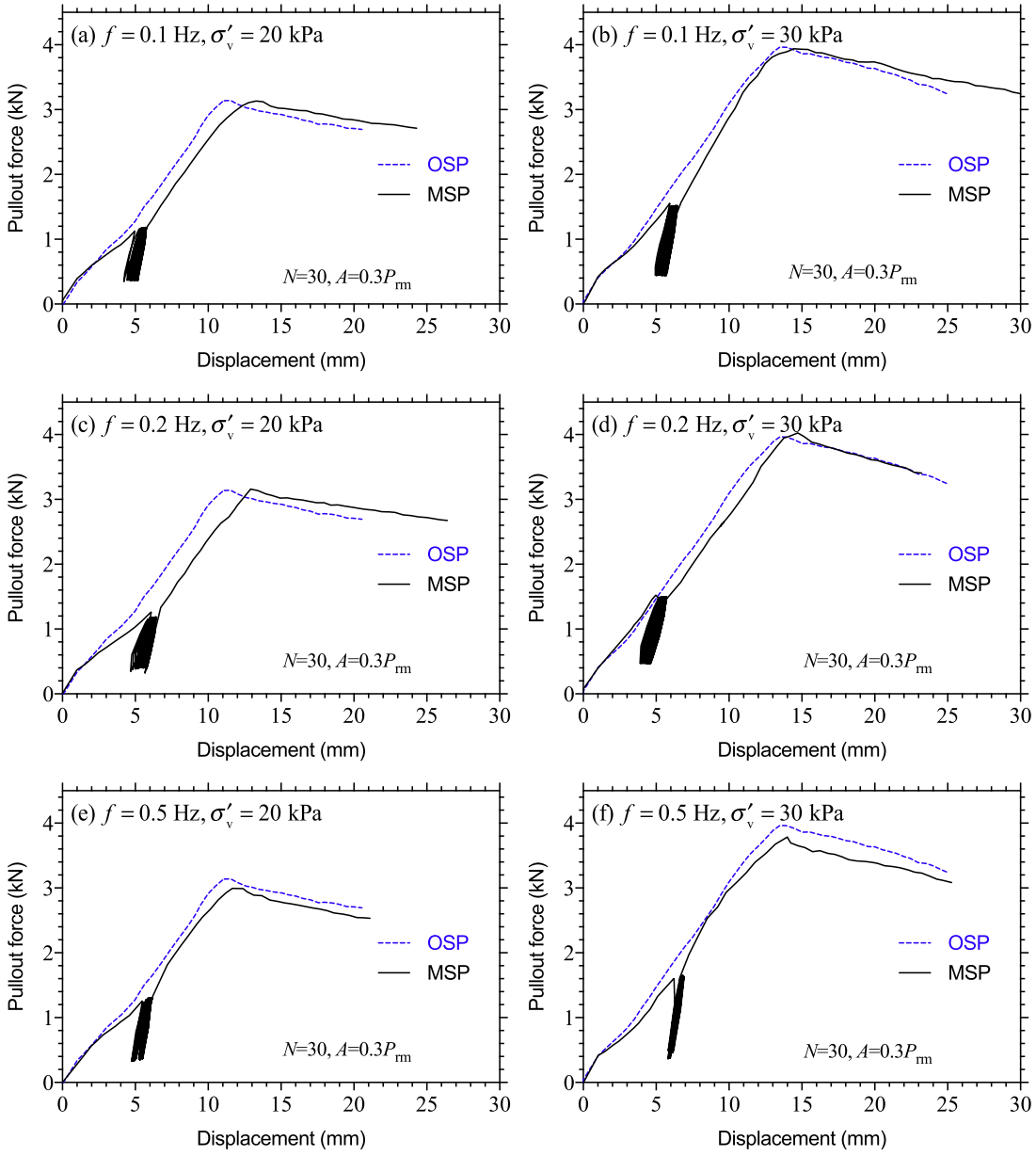

Fig. 5. Multistage pullout test results to study the effect of cyclic tensile load frequency and comparison with one-stage results.

600 mm and a depth of 500 mm to evaluate the factors affecting the values of P_{rc} and $\mu_{s/GSY}$. The test device consists of a linear variable differential transformer (LVDT), a load cell, a hydraulic jack, an airbag, a data acquisition system (DAQ), a computer, an air and oil compressor, a clamping system, and bolts and nuts for fastening the device door. The number of cycles and the values of force and displacement are recorded by the DAQ in real time. Further details on the test apparatus can be found in Mosallanezhad et al. (2017).

2.2. Test materials

PSs with the resistance of T_u = 75.4 kN, length of L = 70 cm, and width of w = 9 cm were used as the reinforcement. These composite strips are made of two different materials: (i) polyester yarn to bear the tensile force, and (ii) a very strong sheath of high-

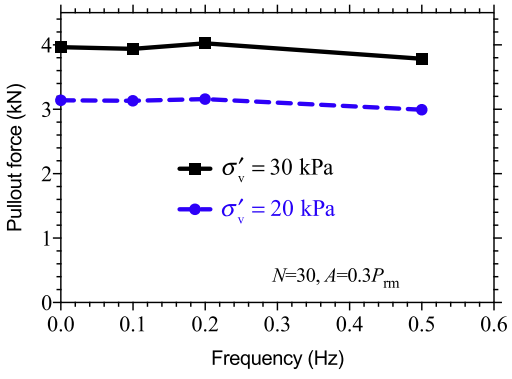

Fig. 6. The pullout resistance under one-stage pullout and post-cyclic conditions versus cyclic tensile load frequency under the vertical effective stresses of 20 kPa and 30 kPa.

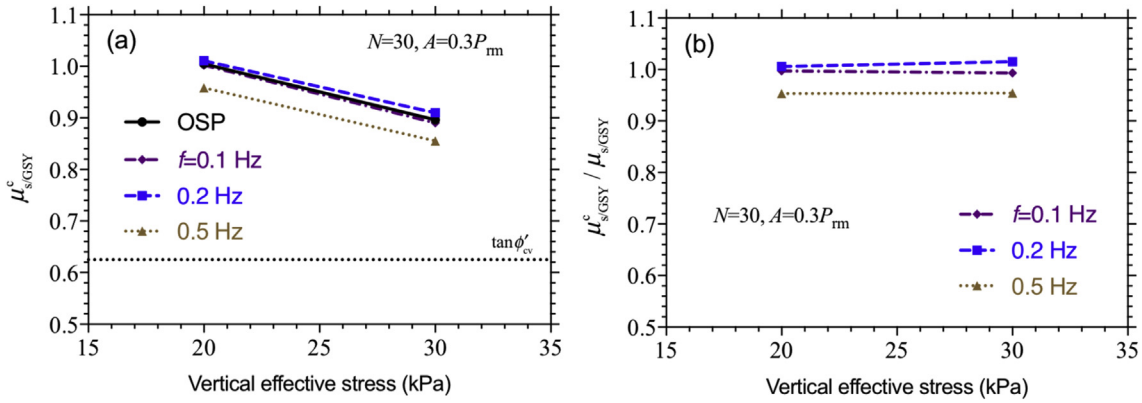

Fig. 7. Effects of the cyclic tensile load frequency and vertical effective stress σ'_v on the peak apparent coefficient of friction $\mu^c_{s/GSY}$ mobilized at the interface in one-stage and post-cyclic conditions.

density polyethylene to withstand environmental (chemical, mechanical, etc.) factors. According to the tensile tests carried out on a PS, the elastic modulus of the PS was estimated as 850 MPa. The loading rate of these tests was 1 mm/min. The basic characteristics of the PS reported by the supplier company are indicated in Table 1.

The test soil is classified as poorly-graded sand according to the unified soil classification system (USCS). The physical properties of the dry soil were determined according to relevant ASTM standards. Based on the standard Proctor compaction test, the maximum dry density and optimum moisture content were

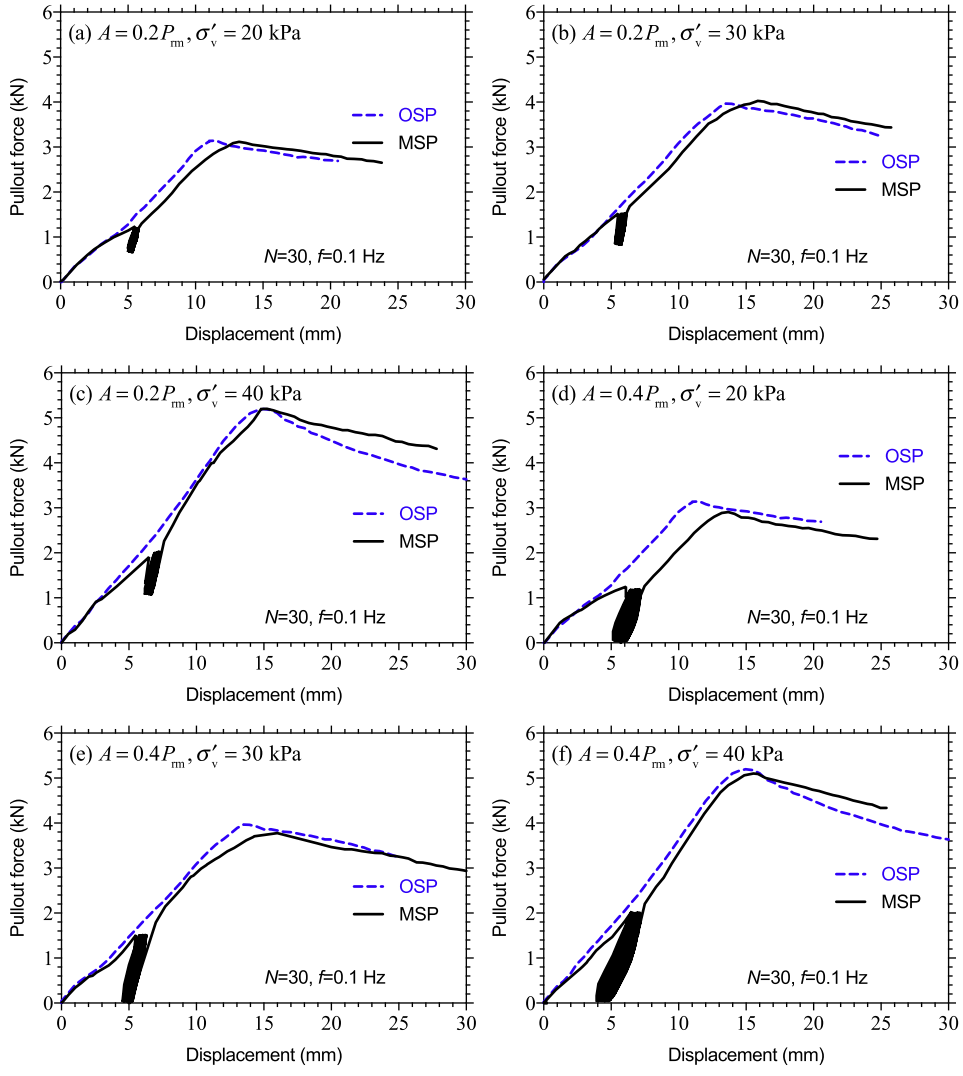

Fig. 8. Multistage pullout test results to study the effect of cyclic tensile load amplitude in comparison with one-stage results.

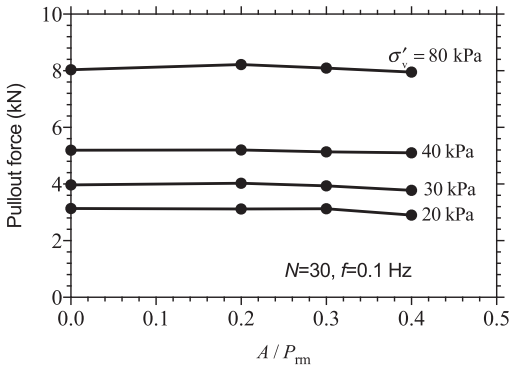

Fig. 9. Pullout resistance under one-stage and post-cyclic conditions versus the cyclic tensile load amplitude under the vertical effective stresses of 20 kPa, 30 kPa, 40 kPa and 80 kPa.

obtained as $\gamma_{dmax} = 1.75$ g/cm^3 and $w_{opt} = 8\%$, respectively. The direct shear tests, conducted at 97% of γ_{dmax} under the vertical effective stresses used in the pullout tests, gave values of the peak (ϕ'_p) and constant volume (ϕ'_{cv}) friction angles about 40° and 32°, respectively. The particle size distribution and compaction curves are depicted in Figs. 1 and 2, respectively. Soil properties are indicted in Table 2.

2.3. Test procedure

The distance between the strips and the sidewalls was $D_S = 25$ cm. Thus, the friction between the soil and the sidewalls was ignored in accordance with ASTM D6706-03 (2003). As shown in Fig. 3, this reinforcement is placed between two layers of compacted dry soil. These layers were compacted in three layers with about 8 cm thickness using a hammer to reach the target dry density of 1.7 g/cm^3, i.e. 97% of γ_{dmax}. In order to obtain uniformly compacted layers, compaction was done by 3 hits of an 8-kg rectangular hammer with dimensions of 300 mm × 200 mm, dropping from a height of 200 mm. Therefore, the energy transferred to the sand is equal to 9600 N m/m^3. Accordingly, approximately 25 cm of compacted soil was located on the PS. One end of the PS was connected to the clamp and the other end was put free on the sublayer soil. The LVDT was utilized to measure the clamp displacement and the load cell was connected between the clamp and the hydraulic jack in order to measure the pullout force. In the next step, the airbag was placed on the soil to apply a uniform and continuous overburden pressure during the tests. The lid of the device was closed and fastened by bolts and nuts. After the air pressure was transferred into the airbag by the compressor and became constant, the LVDT and the load cell were set to initiate the test. Eventually, the hydraulic jack pulled out the reinforcement. The LVDT and the load cell were connected to a central DAQ via a linking wire, and the pullout force, the number of cycles and the clamp displacement were recorded during the pullout process. It should be noted that the clamp system was placed in the box to confine the entire length of the reinforcement during the test (Moraci and Recalcati, 2006). Therefore, the tests without PS (soil-clamp interface) were performed at different vertical effective stresses to deduct the resistance of the clamp from the total resistance of the systems.

According to Table 3, a total of 30 pullout tests, including MSP and one-stage pullout (OSP) tests, and tests carried out without PS (soil-clamp interface), were performed. In the MSP test, the ranges of load frequency and amplitude are 0.1–0.5 Hz and (0.2–0.4)P_{rm}, respectively. The number of load cycles ranges from 30 to 250 and the vertical effective stress varies between 20 kPa and 80 kPa.

2.4. Loading

In this research, OSP and MSP test procedures have been used. The OSP test adopted the same loading procedures as performed by Mosallanezhad et al. (2017). The strip is pulled out at a constant speed of 1 mm/min to achieve the monotonic pullout resistance (P_{rm}), but the MSP test contains three loading phases. According to Fig. 4, in the first phase, the load increases until it reaches the fixed pullout load by using the same constant test rate adopted in static pullout test (1 mm/min). In the next step, the second phase of the MSP test begins as a sinusoidal cycle. To define the load in this section, three parameters including f, A and N must be defined. After the completion of this phase, the third phase continues as same as the first phase to obtain P_{rc}. In fact, in the MSEWs and due to the thrust of the soil, PS reinforcement is under static pullout loads, and seismic loads create an increment of the applied tensile loads. The first and the second phases of the MSP test simulate these conditions. The last phase of the MSP test is performed to investigate the changes in pullout resistance and interface apparent coefficient of friction and to provide a comparison with those values achieved in the conventional OSP tests (Moraci and Cardile, 2009). Several researchers started the cyclic tensile load (second phase of the MSP test) from a fixed index tensile load. For instance, Moraci and Cardile (2009, 2012) started a second phase of the MSP test from a fixed index tensile load varying from 0.2P_{rm} to 0.4P_{rm}; Cardile et al. (2017) used pre-stress tensile load ranging from 0.06P_{rm} to 0.5P_{rm}. A sustained loading history before starting the

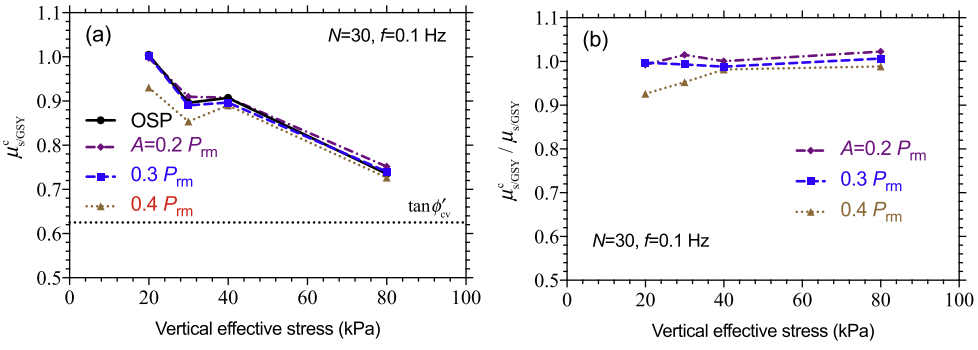

Fig. 10. Effects of the cyclic tensile load amplitude and vertical effective stress σ'_v on the peak apparent coefficient of friction $\mu^c_{s/GSY}$ mobilized at the interface in one-stage and post-cyclic conditions.

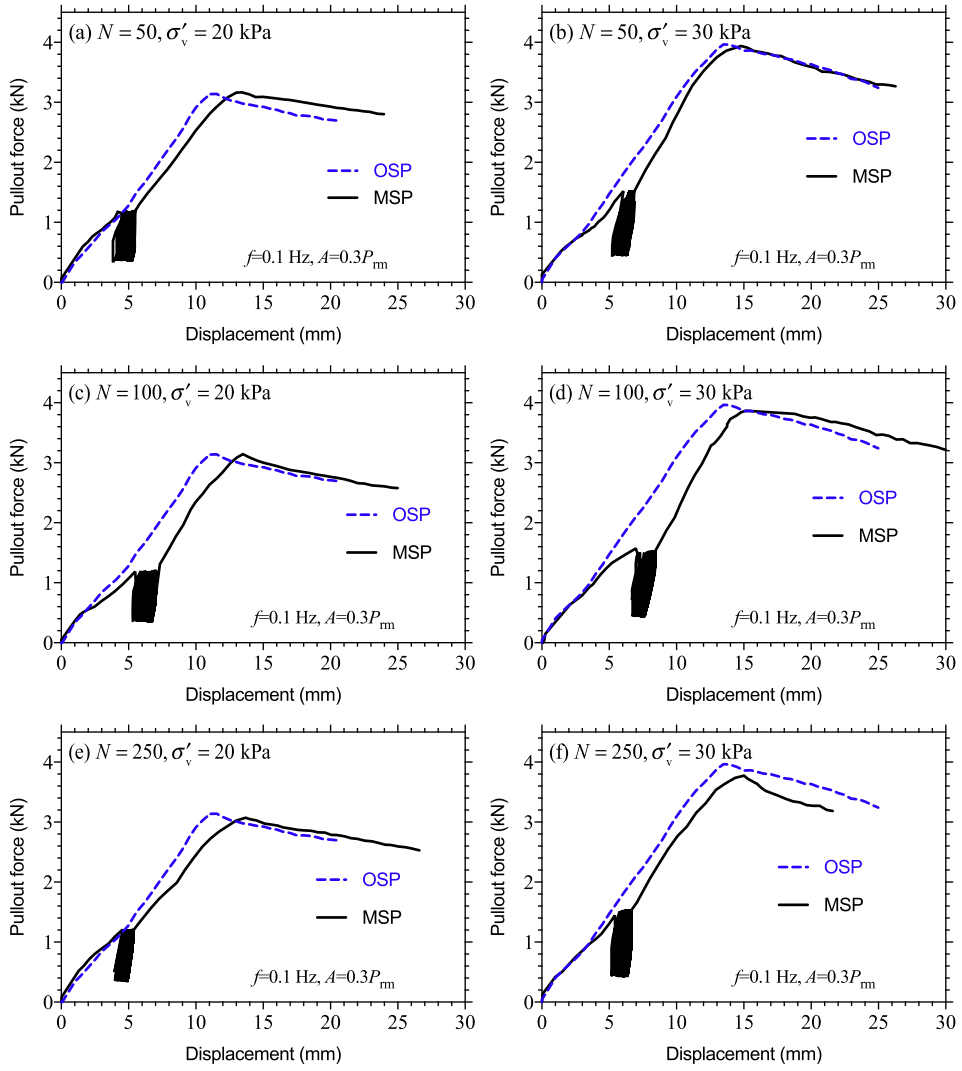

Fig. 11. Multistage pullout test results to study the effect of the number of load cycles and comparison with one-stage results.

cyclic load affects the pullout behavior during the second phase of the MSP test (Kongkitkul et al., 2004). However, the present study aims to investigate the influence of the cyclic loading on the pullout resistance and the peak apparent coefficient of friction mobilized at the soil-PS interface. Thus, the MSP test procedure was used so as to investigate the influences of cyclic loading on the design parameters actually used in the design of earth reinforced structures (Moraci and Cardile, 2009). Therefore, in the present study, all MSP tests were performed with a given loading history ($P_{Fi} = 0.4P_{rm}$).

3. Results and discussion

3.1. Effect of cyclic tensile load frequency

In this series of tests, the load amplitude and the number of cycles were fixed at 0.3P_{rm} and 30, respectively. Three values of frequency (0.1 Hz, 0.2 Hz and 0.5 Hz) were considered. Fig. 5 presents the curves of the MSP and OSP tests under the vertical effective stresses of 20 kPa and 30 kPa. Fig. 6 shows the pullout resistance versus the load frequency for various vertical effective stresses. In each curve, the load frequency of zero indicates the results of the OSP test. As can be observed in Fig. 6, for the values investigated in this research, the load frequency does not have much impact on the pullout resistance, and increase in vertical effective stress leads to an increase in peak pullout resistance. Moreover, changing the frequency up to 0.5 Hz results in a negligible reduction (5%) of pullout resistance. In the post-cyclic pullout conditions, Moraci and Cardile (2009) observed a hardening phenomenon for geogrid embedded in the granular soil at the vertical effective stresses equal to 25 kPa and 50 kPa, whereas at the lower vertical effective stress (10 kPa), a slight softening post-cyclic behavior was reported. Besides, in the monotonic pullout conditions, some reinforcements like geogrids (Abdi and Zandieh, 2014; Yu and Bathurst, 2016), metal strip (Esfandiari and Selamat, 2012), steel grid (Alam et al., 2014) and grid-anchor (Mosallanezhad et al., 2016) do not illustrate a softening behavior. By contrast, in this paper, it is possible to observe that the mechanical response of PS in the post-cyclic conditions was that of softening type for all vertical effective stresses (similar to the OSP test). Furthermore, the unload-reload tensile stiffness at the cyclic phase increases (Fig. 5) due to the viscous characteristic of the PS and different test rates during the second phase of MSP test. Specifically, in order to maintain the imposed load frequency and amplitude, the test rate has to be varied during the single load cycle, reaching a displacement rate

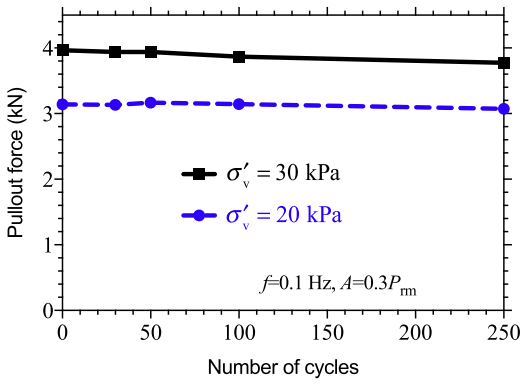

Fig. 12. The pullout resistance under one-stage and post-cyclic conditions versus the number of load cycles under the vertical effective stresses of 20 kPa and 30 kPa.

higher than the monotonic displacement rate. The higher test rate leads to a higher tensile stiffness response of the PS. After this phase, the tensile stiffness decreases to the values obtained in the OSP tests.

Fig. 7 shows the variations of $\mu^c_{s/GSY}$ and $\mu^c_{s/GSY}/\mu_{s/GSY}$ with vertical effective stress. It is observed that the values of $\mu_{s/GSY}$ with a frequency of 0.5 Hz are slightly lower than the rest of other frequencies. The monotonic peak apparent coefficient of friction $\mu_{s/GSY}$ mobilized at the soil-PS interface decreases with the increase in vertical effective stress (Lo, 1998, 2003). Similarly, in addition to $\mu_{s/GSY}$, the results show that by increasing the vertical effective stress, $\mu^c_{s/GSY}$ also decreases due to dilatancy at the interface (Moraci and Cardile, 2009). It should be noted that for the selected parameters in this figure, the values of $\mu^c_{s/GSY}$ and $\mu_{s/GSY}$ are always higher than the coefficients of friction mobilized in the sand at constant volume conditions $\tan\phi'_{cv} = 0.625$ (Fig. 7a). As can be seen in Fig. 7b, the values of $\mu^c_{s/GSY}/\mu_{s/GSY}$ are very close to unity, which means that the effect of the load frequency on the values of the peak apparent coefficient of friction mobilized at the soil-PS interface is negligible, while for geogrid, based on the results of Moraci and Cardile (2009), the second phase of the MSP test leads to a decrease in post-cyclic peak interface apparent coefficient of friction mobilized at the interface, varying from 0.11 to 0.16, at frequency of 0.1 Hz.

3.2. Effect of cyclic tensile load amplitude

In this section, load frequency and number of cycles were fixed at 0.1 Hz and 30, respectively. Load amplitude A was considered as 0.2P_{rm}, 0.3P_{rm} and 0.4P_{rm}. The results of MSP and OSP tests, in terms of the peak pullout resistance, are presented in Fig. 8. In Fig. 9, the relationships of pullout resistance versus A/P_{rm} are plotted for different vertical effective stresses. Note that $A/P_{rm} = 0$ corresponds to the results of the OSP test. It can be seen that P_{rc} decreases slightly with the increase in A/P_{rm}. It should be noted that the differences between P_{rm} and P_{rc} for the vertical effective stresses of 20 kPa, 30 kPa, 40 kPa and 80 kPa are 7%, 9%, 2% and 2%, respectively. In geogrid, the cyclic tensile load amplitude affects the pullout resistance at the applied vertical effective stress higher than 50 kPa, whereas at the lower vertical effective stress, this influence can be ignored (Moraci and Cardile, 2009). By contrast, in the PS, the cyclic tensile load amplitude does not have a significant effect on the pullout resistance at all applied vertical effective stresses in this study. Besides, the unload-reload tensile stiffness evaluated at the cyclic phase in the MSP tests is very high. In the third phase of the MSP test (performed at constant displacement rate of 1 mm/min), the tensile stiffness decreases to the values obtained in the OSP tests. Moreover, the softening behavior can be observed from the values obtained under OSP and MSP conditions. Fig. 9 shows that the influence of the cyclic tensile load amplitude on the pullout resistance seems to be negligible.

The variations of $\mu^c_{s/GSY}$ and $\mu^c_{s/GSY}/\mu_{s/GSY}$ with vertical effective stress are shown in Fig. 10a. As can be observed in this figure, also in this case, the monotonic and the post-cyclic peak apparent coefficients of friction mobilized at the soil-PS interface decrease as the vertical effective stress increases. In addition, $\mu^c_{s/GSY}$ and $\mu_{s/GSY}$ are higher than the coefficient of friction mobilized in the sand in critical state ($\tan\phi'_{cv}$). Experimental results depict that the effect of the cyclic tensile load amplitude on the values of $\mu_{s/GSY}$ can be ignored (Fig. 10b).

3.3. Effect of number of load cycles

The experimental results related to the effect of number of cycles are presented in Fig. 11. In this figure, the cyclic tensile load frequency and amplitude were considered as 0.1 Hz and 0.3P_{rm}, respectively. The number of cycles was considered as 30, 50, 100 and 250. In the figures of this section, the softening behavior is in accordance with that obtained in the OSP test. Moreover, in this case, the unload-reload tensile stiffness at the second phase of the MSP test rises (Fig. 11), and then it decreases to the values obtained in the OSP test. The maximum differences in the pullout resistance due to the change in the number of cycles are insignificant, which are 2% and 5% at the vertical effective stresses of 20 kPa and 30 kPa, respectively (Fig. 12). In Fig. 12, the case $N = 0$ indicates the results of the OSP test. As can be seen in Figs. 12 and 5a, b, with increasing number of cycles from 30 to 250, the pullout resistance gradually decreases. Moreover, monotonic and post-cyclic pullout resistances increase with the increase in vertical effective stress. According to

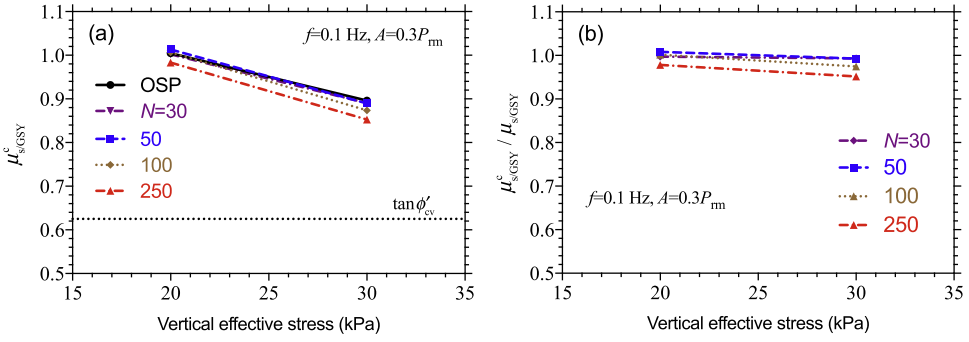

Fig. 13. The effect of the number of load cycles and vertical effective stress σ'_v on the peak apparent coefficient of friction $\mu^c_{s/GSY}$ mobilized at the interface in one-stage and post-cyclic conditions.

Fig. 13, it can be observed that similar to the OSP test, the values of $\mu^{c}_{s/GSY}$ in the MSP test decrease with the increase in vertical effective stress. Furthermore, the ratios of $\mu^{c}_{s/GSY}/\mu_{s/GSY}$ are close to unity. Thus, the number of cycles also has a negligible effect on the peak apparent coefficient of friction mobilized at the soil-PS interface.

4. Conclusions

In order to evaluate the post-cyclic behavior of PS buried in compacted sandy soil, MSP tests were conducted. The effects of various factors such as cyclic tensile load frequency and amplitude, number of load cycles and vertical effective stress on the post-cyclic pullout resistance and the post-cyclic peak apparent coefficient of friction mobilized at the soil-PS interface were investigated. The following conclusions were drawn:

(1) Similar to OSP test, the post-cyclic peak apparent coefficient of friction mobilized at the soil-PS interface ($\mu^{c}_{s/GSY}$) decreases with the increase in vertical effective stress. The post-cyclic pullout resistance also increases with the increase in vertical effective stress.
(2) Within the values investigated, the cyclic tensile load frequency has no effect on the pullout resistance and the values of $\mu^{c}_{s/GSY}$. By changing the frequency (from 0.1 Hz to 0.5 Hz), the values of $\mu^{c}_{s/GSY}$ are always higher than the friction mobilized in the sand in the critical state ($\tan\phi'_{cv}$).
(3) For the values studied, the effect of the cyclic tensile load amplitude is insignificant. The post-cyclic peak apparent coefficient of friction mobilized at the soil-PS interface is higher than the coefficient of friction of the soil at constant volume conditions.
(4) Changing the number of cycles from 30 to 250 causes slight changes in the pullout resistance and the peak apparent coefficient of friction mobilized at the soil-PS interface.
(5) The differences between the post-cyclic pullout resistance (P_{rc}) and the monotonic pullout resistance (P_{rm}) are insignificant in this study. In other words, the post-cyclic pullout behavior of the PS is as same as its monotonic behavior.

Conflicts of interest

The authors wish to confirm that there are no known conflicts of interest associated with this publication and there has been no significant financial support for this work that could have influenced its outcome.

References

Abdi M, Arjomand M. Pullout tests conducted on clay reinforced with geogrid encapsulated in thin layers of sand. Geotextiles and Geomembranes 2011;29(6):588–95.
Abdi M, Zandieh A. Experimental and numerical analysis of large scale pull out tests conducted on clays reinforced with geogrids encapsulated with coarse material. Geotextiles and Geomembranes 2014;42(5):494–504.
Alam MJI, Lo S, Karim M. Pull-out behaviour of steel grid soil reinforcement embedded in silty sand. Computers and Geotechnics 2014;56:216–26.
ASTM D6706-03. Standard test method for measuring geosynthetic pullout resistance in soil. West Conshohocken, PA,USA: ASTM International; 2003.
Bathurst R, Hatami K. Seismic response analysis of a geosynthetic-reinforced soil retaining wall. Geosynthetics International 1998;5(1–2):127–66.
Cai Z, Bathurst RJ. Seismic response analysis of geosynthetic reinforced soil segmental retaining walls by finite element method. Computers and Geotechnics 1995;17(4):523–46.
Cardile G, Moraci N, Pisano M. Tensile behaviour of an HDPE geogrid under cyclic loading: experimental results and empirical modelling. Geosynthetics International 2017;24(1):95–112.
Esfandiari J, Selamat M. Laboratory investigation on the effect of transverse member on pull out capacity of metal strip reinforcement in sand. Geotextiles and Geomembranes 2012;35:41–9.
Kongkitkul W, Hirakawa D, Tatsuoka F, Uchimura T. Viscous deformation of geosynthetic reinforcement under cyclic loading conditions and its model simulation. Geosynthetics International 2004;11(2):73–99.
Latha GM, Krishna AM. Seismic response of reinforced soil retaining wall models: influence of backfill relative density. Geotextiles and Geomembranes 2008;26(4):335–49.
Ling H, Leshchinsky D, Perry E. Seismic design and performance of geosynthetic-reinforced soil structures. Géotechnique 1997;47(5):933–52.
Ling H, Leshchinsky D, Chou NN. Post-earthquake investigation on several geosynthetic-reinforced soil retaining walls and slopes during the Ji-Ji earthquake of Taiwan. Soil Dynamics and Earthquake Engineering 2001;21(4):297–313.
Liu F, Wang P, Geng XY, Wang J, Lin X. Cyclic and post-cyclic behaviour from sand–geogrid interface large-scale direct shear tests. Geosynthetics International 2015;23(2):129–39.
Lo S. Pull-out resistance of polyester straps at low overburden stress. Geosynthetics International 1998;5(4):361–82.
Lo S. The influence of constrained dilatancy on pullout resistance of strap reinforcement. Geosynthetics International 2003;10(2):47–55.
Moraci N, Cardile G. Influence of cyclic tensile loading on pullout resistance of geogrids embedded in a compacted granular soil. Geotextiles and Geomembranes 2009;27(6):475–87.
Moraci N, Cardile G. Deformative behaviour of different geogrids embedded in a granular soil under monotonic and cyclic pullout loads. Geotextiles and Geomembranes 2012;32:104–10.
Moraci N, Recalcati P. Factors affecting the pullout behaviour of extruded geogrids embedded in a compacted granular soil. Geotextiles and Geomembranes 2006;24(4):220–42.
Mosallanezhad M, Bazyar MH, Saboor MH. Novel strip-anchor for pull-out resistance in cohesionless soils. Measurement 2015;62:187–96.
Mosallanezhad M, Sadat Taghavi SH, Khadiv Sarvestani M. Large-scale pullout testing of a new 'rooted' geogrid. International Journal of Physical Modelling in Geotechnics 2017;17(3):195–203.
Mosallanezhad M, Taghavi SS, Hataf N, Alfaro M. Experimental and numerical studies of the performance of the new reinforcement system under pull-out conditions. Geotextiles and Geomembranes 2016;44(1):70–80.
Nouri H, Fakher A, Jones C. Development of horizontal slice method for seismic stability analysis of reinforced slopes and walls. Geotextiles and Geomembranes 2006;24(3):175–87.
Nova-Roessig L, Sitar N. Centrifuge model studies of the seismic response of reinforced soil slopes. Journal of Geotechnical and Geoenvironmental Engineering 2006;132(3):388–400.
Palmeira EM. Bearing force mobilisation in pull-out tests on geogrids. Geotextiles and Geomembranes 2004;22(6):481–509.
Palmeira EM. Soil-geosynthetic interaction: modelling and analysis. Geotextiles and Geomembranes 2009;27(5):368–90.
Panah AK, Yazdi M, Ghalandarzadeh A. Shaking table tests on soil retaining walls reinforced by polymeric strips. Geotextiles and Geomembranes 2015;43(2):148–61.
Suksiripattanapong C, Horpibulsuk S, Chinkulkijniwat A, Chai JC. Pullout resistance of bearing reinforcement embedded in coarse-grained soils. Geotextiles and Geomembranes 2013;36:44–54.
Tang QR, Hua JM, Zhou J. Seismic dynamic response of geosynthetic-reinforced soil segmental retaining wall. Electronic Journal of Geotechnical Engineering 2013;18:1831–46.
Yu Y, Bathurst RJ. Influence of selection of soil and interface properties on numerical results of two soil-geosynthetic interaction problems. International Journal of Geomechanics 2016;17(6). https://doi.org/10.1061/(ASCE)GM.1943-5622.0000847.

Dr. Amin Keshavarz is currently an associate professor of Civil Engineering at School of Engineering of Persian Gulf University, Iran. He received his BSc degree in Civil Engineering from Persian Gulf University in 1997. He also received his MSc and PhD degrees in Civil Engineering (Soil Mechanics and Foundations) from Shiraz University, Iran in 2000 and 2007, respectively. His research interests cover stress characteristics and zero extension lines (ZEL) methods, soil dynamics and geotechnical earthquake engineering, and stability analysis of reinforced and unreinforced soil slopes and retaining walls.